Dielectric properties and lattice dynamics of Ca-doped $K_{0.95}Li_{0.05}TaO_3$

S. Wakimoto*
Quantum Beam Science Directorate, Japan Atomic Energy Agency, Tokai, Ibaraki 319-1195, Japan.

G. A. Samara, R. K. Grubbs and E. L. Venturini
Sandia National Laboratories, Albuquerque, New Mexico 87185, USA

L. A. Boatner
Oak Ridge National Laboratory, Oak Ridge, Tennessee 37831, USA

G. Xu and G. Shirane †
Department of Physics, Brookhaven National Laboratory, Upton, New York 11973, USA

S.-H. Lee
NIST Center for Neutron Research, National Institute of Standards and Technology, Gaithersburg, MD 20899 and Department of Physics, University of Virginia, Charlottesville, VA22904, USA

(Dated: February 6, 2008)

Relaxor behavior and lattice dynamics have been studied by employing dielectric measurements and neutron scattering methods for a single crystal of $K_{1-x}Li_xTaO_3$ ($x = 0.05$), where a small amount of a Ca impurity (~ 15 ppm) was incorporated during the single crystal growth procedure. The dielectric constant $\epsilon'(\omega, T)$ shows qualitatively similar behavior to that of Ca-free KLT with $x = 0.043$ with both compositions exhibiting relaxational properties with no evidence for a ferroelectric transition. The absolute value of $\epsilon'(\omega, T = 0)$ for the present crystal is larger by an order of magnitude than that of the Ca-free sample due to charge carriers induced by the Ca doping. This large value is shown to be due to a Maxwell-Wagner relaxation process associated with the low temperature (< 8 K) activation of frozen electronic carriers. The dielectric loss tangent $\tan\delta$ reveals three Debye-like relaxations with Arrhenius activation energies of 80, 135, and 240 meV that are assigned to Li^+ dipoles, Ca^{2+}-related relaxation and the Li^+-Li^+ dipolar pairs, respectively. In the neutron scattering results, diffuse scattering ridges appear around the nuclear Bragg peaks along the [100] direction below ~ 150 K and phonon line broadening features start to appear at even higher temperatures suggesting that polar nano-regions (PNR's) start to form at these temperatures. These results are supported by the dielectric data that reveal relaxor behavior starting at ~ 200 K on cooling. From analyses of the diffuse intensities at different zones, we have derived atomic displacements in the PNR's. The results suggest that the displacements include a uniform phase shift of all of the atoms in addition to the atomic displacements corresponding to a polarization vector of the transverse optic soft ferroelectric mode, a finding that is analogous to that in the prototypical relaxor material $Pb(Mg_{1/3}Nb_{2/3})O_3$.

I. INTRODUCTION

Relaxor ferroelectrics that have a relatively large dielectric permittivity over a wide temperature range have attracted a significant amount of attention due to their high potential for device applications as well as their scientific challenges. It is now widely believed that relaxor behavior, whose universal signature is a frequency(ω)-dependent peak in the dielectric constant $\epsilon'(\omega, T)$, arises from the relaxational nature of randomly-oriented polarized nano-regions (PNR's). However, the mechanism for the PNR formation is not fully understood yet. In particular, unlike the case for displacive ferroelectric materials, possible contribution of the zone-center transverse optic (TO) soft phonons to the PNR condensation still remains to be clarified.

The relaxor material system $K_{1-x}Li_xTaO_3$ (KLT(x)) provides a unique opportunity for systematic research ranging from a relaxor state in the material at low Li concentrations to a ferroelectric state at high concentrations. The parent compound $KTaO_3$ is an incipient ferroelectric material that does not undergo a ferroelectric transition[1] although the TO soft mode softens remarkably at low temperature.[2] On substituting at the K^+ site, the much smaller Li^+ ion occupies an off-center positions resulting in a large dipole moment that is the precursor for PNR formation on cooling. At high Li concentration, the PNR's percolate, and the system achieves ferroelectric order.

Although the system KLT(x) has been studied extensively by Raman scattering,[3,4,5] and its soft mode character is well-established, only a few neutron scattering studies have been carried out mainly to explore the role of the soft mode of the host crystal in the formation and growth of the PNR's. Yong *et al.*[6] have studied the dif-

†Deceased.

fuse neutron scattering in KLT that originates from PNR formation. They reported a strong diffuse intensity at (110) and its absence at both (100) and (200). If we assume a PNR condensation from the TO soft mode as in the case of the ordinary ferroelectrics, then the structure factors for the diffuse and the inelastic scattering by the TO mode should agree. However, it is found that the inelastic structure factor for the TO soft mode of KLT at (200) is much larger than that at (110) in disagreement with the diffuse scattering intensities.

Such disagreements between the diffuse intensities and inelastic structure factors have also been reported in the relaxor material $Pb(Mg_{1/3}Nb_{2/3})O_3$ (PMN).[7] Moreover, in this latter case, the atomic displacements determined from the diffuse intensities at several zones do not conserve the center-of-mass (CM).[8] These facts suggest an apparent disconnection between the PNR condensation and the soft phonon mode in PMN. However, Hirota *et al.*[9] have reconciled these two observations by introducing a model of the soft mode condensation that incorporates an *additional uniform phase shift*, in which the total atomic displacements can be divided into two components. One component originates from the normal condensation of the TO soft mode that conserves the CM, and the other component represents a uniform shift of all of the atoms in the polarization direction.

In the present paper, we report and discuss dielectric and neutron scattering experiments performed on KLT with $x = 0.05$. The results provide detailed views of the response and physics of this crystal. An additional objective is to determine if the anomalous lattice dynamical features observed in the prototypical relaxor PMN are common to other ABO_3 relaxors. This comparison offers us a unique opportunity to compare two different types of relaxors, one is KLT in which off-center impurity ions trigger a local polarization (PNR's) on the incipient ferroelectric background, and the other is PMN in which random occupation of the B-sites by two different ions with different valences produces the disorder that breaks long-range ferroelectric (FE) correlations and order resulting in the formation of a relaxor (R) state.

II. EXPERIMENTAL DETAILS

The KLT samples used in the present study were $< 100 >$ oriented single crystals cut from one boule that was grown by solidification from the melt. The boule was nominally undoped, but our dielectric measurements (to be presented below) suggested the presence of an unintentional dopant leading to some electronic conduction and a high dielectric loss. Subsequent analysis revealed the presence of only Ca impurity (at a level of ~ 15 ppm) in the starting powder used in the crystal growth.[10] Clearly, some of the Ca was incorporated into the crystal, but at a sufficiently low level that was difficult to quantify. The crystal was colorless with no indication of any significant free carrier absorption that usually produces a blue coloration in more highly conducting crystals of this type. Although the Ca dopant had a definite influence on the dielectric properties, normally it would not be expected to have a significant influence on the lattice dynamics measured by neutron scattering.

It is well established that not all of the Li in the starting mixture of the oxides is incorporated into the growing crystal during the solidification process due to segregation coefficient effects. It is estimated that 35 % of the Li content in the growth charge is incorporated.[11] The Li composition of our KLT crystal ($\simeq 5$ at.%) was estimated from the amount of Li in the melt and from the established relationship between the peak temperature in the $\epsilon'(T)$ response and the Li content.[12] Henceforth we shall designate our composition as KLT(5):Ca.

For the dielectric measurements, the large (100) faces of the crystal were polished using colloidal silica and were subsequently covered with vapor-deposited chromium followed by gold. The sample was investigated by dielectric spectroscopy with measurements of the real (ϵ') and loss ($\tan\delta$) parts of the dielectric function performed as functions of temperature (4−300 K), frequency ($10^2 - 10^6$ Hz) and hydrostatic pressure ($0 - 7.5$ kbar). The pressure system consisted of a compressor and an intensifier that fed the pressure-transmitting medium (helium gas) into a cell placed in a low temperature Dewar. The pressure was measured using a calibrated manganin gauge to an accuracy of better than 4%.

The neutron scattering experiments were performed using triple axis spectrometers SPINS at NIST, LTAS at JAEA, and TAS1 at JAEA. The diffuse scattering was measured at SPINS and LTAS with an incident neutron energy of $E_i = 5$ meV ($\lambda = 4.04$ Å) and a collimation sequence: Guide-80′-S-80′-open (S denotes the sample), and also at TAS1 with $E_i = 14.7$ meV ($\lambda = 2.36$ Å) and 40′-40′-S-40′-80′. The phonon modes were studied at TAS1 with a fixed final energy of $E_f = 14.7$ meV and 40′-40′-S-80′-open. Beryllium and pyrolytic graphite filters were utilized for the measurements with $\lambda = 4.04$ Å and $\lambda = 2.36$ Å, respectively, to remove those neutrons with higher harmonic wavelength ($\lambda/2, \lambda/3, etc.$).

A KLT(5):Ca crystal with dimensions of $6 \times 10 \times 13$ mm^3, cut from the same crystal boule that was used for the dielectric measurements, was prepared for the neutron scattering experiments. The crystal was mounted in an unstrained manner on an aluminum post using aluminum foil, and the aluminum post was then masked by a cadmium plate to avoid any scattering from it. The sample was sealed in an aluminum can filled with He gas, and placed in a He-gas closed-cycle refrigerator with the [100] and [010] axes in the horizontal scattering plane. In the temperature range $10 \leq T \leq 295$ K, the crystal structure was cubic as evidenced in the neutron scattering resolution, with a lattice constant 3.95 Å, corresponding to a reciprocal lattice unit (r.l.u.) of 1.59 Å^{-1}.

III. Li AND Ca SUBSTITUTION IN $KTaO_3$

Before presenting the dielectric and lattice dynamics properties, we briefly review in this section the effects of Li and Ca substitution on $KTaO_3$.

The substitution of Li^+ for K^+ in KLT raises an immediate issue. The K^+ ion has a radius r_i of 1.3 Å and fits well in the lattice, occupying a centrosymmetric position in the oxygen ion cage that surrounds it in $KTaO_3$ (Fig. 1 (a)). The Li^+ ion, on the other hand, is too small ($r_i = 0.68$Å), and the oxygen cage dimension is too large in comparison. This is a circumstance that occurs relatively often in solids with the expected consequence that the small ion will shift to an off-center position. This is expected for Li in KLT, and indeed, this effect was observed early on.[12,13,14] The shift, as expected from the lattice symmetry, is in the [100] direction (Fig. 1 (b)) and is quite large (1.2 Å).[13] In this off-center position, the Li^+ ion has a relatively large dipole moment, which can interact with neighboring Li dipoles. Additionally, because of the high polarizability of the $KTaO_3$ host, the Li dipole can polarize adjacent unit cells resulting in polar nano-regions. These are precisely the conditions that lead to dipolar glass and relaxor behavior. Indeed, this is what is observed experimentally.[12,13]

Leung[15] has performed a first-principles study of Ca^{2+} substitution in $KTaO_3$. Although his study is for $KTaO_3$ and not on KLT, we believe that the results are relevant to our Ca-doped KLT crystals. The results show that Ca^{2+} substitutes at both the K^+ and Ta^{5+} sites. At the K^+ site, the Ca antisite, Ca_K^+, would be expected to produce a K vacancy, but Leungs results find this circumstance highly unfavorable energetically. Thus, the Ca^{2+} simply donates an electron. At the Ta^{5+} site, the Ca^{2+} binds to an oxygen vacancy (V_O), thereby forcing the Ca^{2+} off-center and resulting in a dipolar complex. (Oxygen vacancies are formed on Ca^{2+} substitution to preserve charge neutrality, and they are also native defects in perovskites). The calculations predict that the activation energy for the reorientation of the (Ca-V_O) dipole via oxygen-vacancy hopping within the first neighbor shell exceeds 2 eV. This large energy precludes the direct involvement of the (Ca-V_O) complex in the observed new relaxations that have much lower activation energies in the present KLT crystals. (See the next section.)

Early work[1,16] on Ca-doped $KTaO_3$ (KT) has suggested that the Ca is fully ionized at room temperature. Presuming that Ca^{2+} substitutes at the K^+ site, Senhouse *et al.*[16] showed that the net ionized donor concentration is equal to the Ca concentration. These results would suggest that most of the Ca^{2+} resides at the K^+ site. However, impurities and defects (primarily oxygen vacancies that are prominent defects in ABO_3 oxides and in Ca-doped KT[14]) can also be sources of free electrons. Wemple[1] also showed that there is no "freeze-out" of the Ca-generated electrons in KT down to temperatures approaching liquid helium temperature.

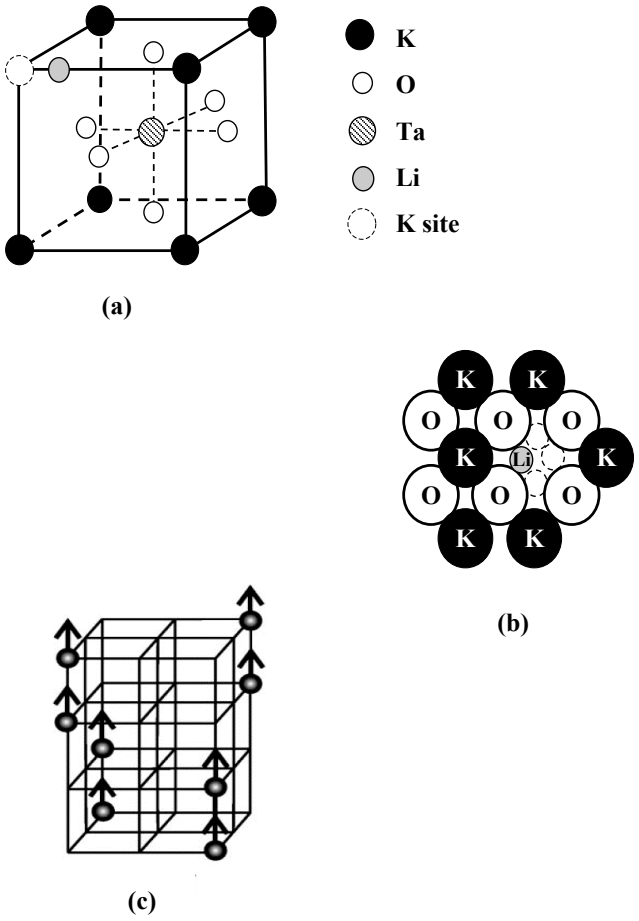

FIG. 1: (a) The ABO_3 structure of KLT showing the off-center position of the Li ion at the K site. The Li^+ hops among 6 equivalent positions, 4 of which are shown in (b). (c) shows the configuration of the co-linear Li^+-Li^+ ion pairs.

When present in sufficient concentrations ($>\sim 10^{17}/cm^3$) the Ca-generated free electrons in Ca-doped KT and related crystals produce free carrier absorption and an associated blue coloration. In our present KLT(5):Ca crystal the Ca was present in small amounts, and consequently these crystals were colorless - containing relatively few free electrons and no noticeable free carrier absorption. However, this small amount of Ca had a significant influence on the amplitude of dielectric response and also a minor influence on the lattice dynamics. (See later discussion.)

IV. RESULTS AND DISCUSSION

A. Dielectric response

Figure 2 shows the dielectric response of our KLT(5):Ca crystal at 1 bar. The inset in Fig. 2(a) shows $\epsilon'(\omega, T)$ for an undoped 4.3 at.% Li KLT crystal[17] - a composition whose dielectric response is seen to

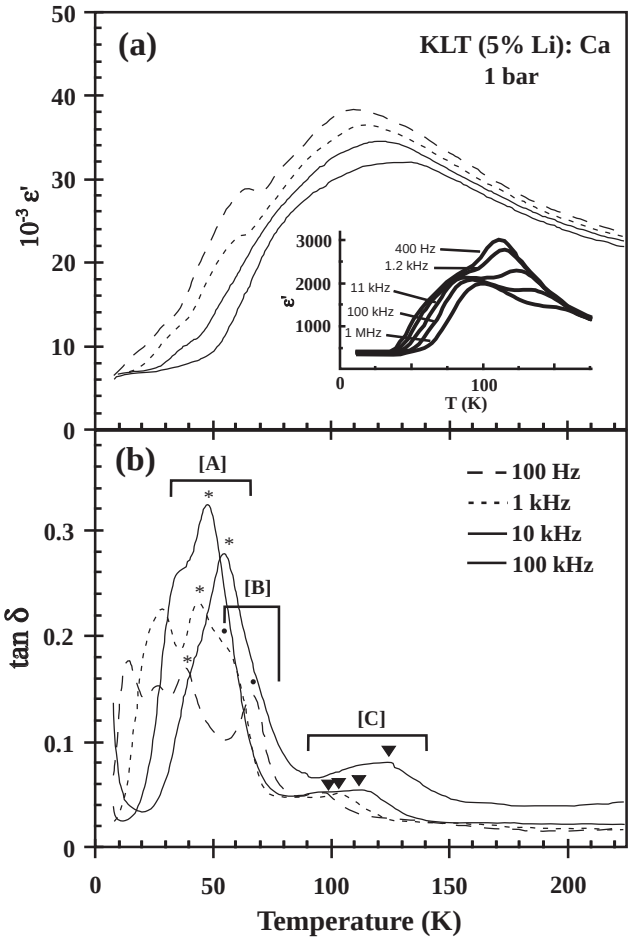

FIG. 2: The 1 bar ϵ' and $\tan\delta$ responses of the KLT(5):Ca crystal. The inset is the response of undoped KLT(4.3) according to Prosandeev *et al.* (Ref. 17.) Three primary relaxations denoted by A, B and C are noted in (b).

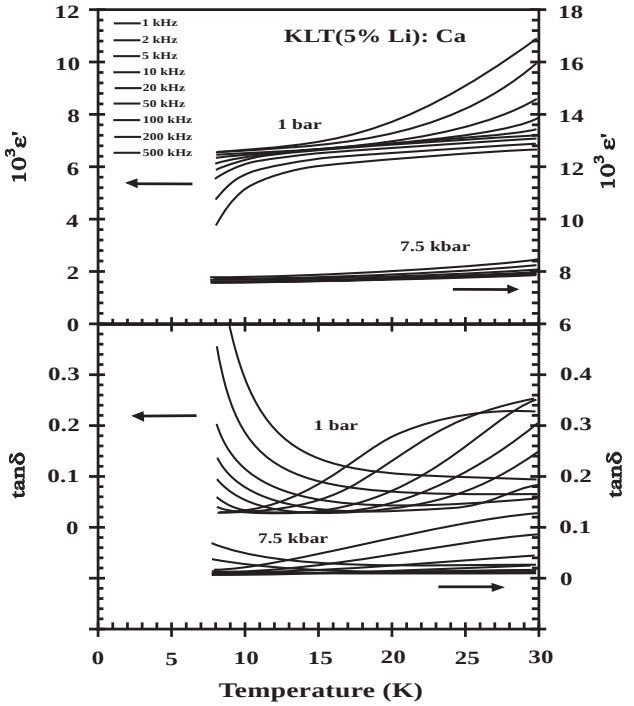

FIG. 3: Low T dielectric response at 1 bar and 7.5 kbar hints at the onset of a low T (< 8 K) relaxation in KLT(5):Ca.

be very close to KLT(5). The main overlapping peaks in this relaxational response are associated with the relaxations of isolated Li^+ dipoles (at the lower temperature) and with (Li^+ - Li^+) ion pairs with kinetic parameters $E \sim 80(240)$ meV and $\omega_o \sim 1.5\times10^{12}$ s^{-1} (7×10^{14} s^{-1}), respectively.[17,18,19] The relaxational dielectric response of our KLT(5):Ca crystal in Fig. 2(a) has some similarities to that in the inset, but there are important differences.

Starting at low temperatures, we note that the amplitude of ϵ' below $\sim$ 20 K ($\sim$ 6000) is over an order of magnitude larger than that of the undoped KLT crystal of about the same Li concentration as shown in the inset in Fig. 2 (a). This strong low-T enhancement of ϵ' in KLT(5):Ca is due to the Ca^{2+} doping. A feature in the KLT(5):Ca data in Fig. 2, namely a relaxational feature below 10 K, points to the mechanism for this enhancement. This feature is shown in Fig. 3. The onset of this relaxation is reflected in the simultaneous highly dispersive decrease in ϵ' and increase in $\tan\delta$ at 1 bar. This relaxation is accompanied by strong frequency dispersion in both $\epsilon'(T)$ and $\tan\delta(T)$, a step in $\epsilon'(T)$ with ϵ' increasing from $\sim$ 600 at the lowest temperatures (the expected value for this composition in the absence of Ca [See inset in Fig. 2 (a)]) to $\sim$ 6000 at the plateau region, and a large peak in $\tan\delta(T)$. These features are the signature of a capacitive barrier layer that, for our present case, could be due to either a Schottky barrier or space charge accumulation at the metal contacts.[20]

We speculate that the relaxation is, in fact, associated with the activation of the Ca-donated free carriers (electrons). Specifically, the carriers are frozen at the lowest temperatures and are activated at the onset of the relaxation. To check this hypothesis, we have measured the dc resistivity (ρ) of our crystal (using In/Ga eutectic as contacts). The results in Fig. 4 show that above the relaxation: $\rho < 10^5$ Ω cm, but that it increases sharply by over 3 orders of magnitude below 8 K, clear evidence of carrier freeze-out. These results also support Wemples[1] early finding for $KTaO_3$:Ca that carrier freeze-out occurs only at the lowest temperatures. The dielectric measurements were repeated at a pressure of 7.5 kbar. Pressure suppresses the frequency dispersion and shifts the relaxation to lower temperatures. It also increases the amplitude of $\epsilon'(T)$ in the plateau region by 15 % under 7.5 kbar. In early high pressure work on KT and other perovskites, Wemple *et al.*[21] concluded that for these materials the electron mobility is related to ϵ' by the relationship $\mu \propto 1/\epsilon' + constant$. Since ϵ' decreases with pressure as a result of the increase in soft mode frequency, μ can be expected to increase leading to an

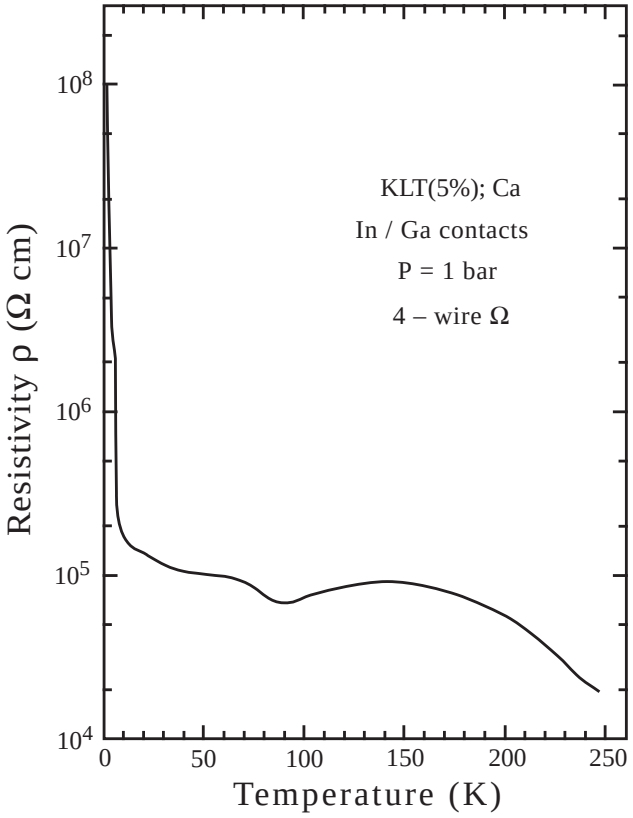

FIG. 4: The temperature dependence of the resistivity, $\rho(T)$, of KLT(5):Ca showing carrier (electron) freeze-out below 10 K. It is the un-freezing of the carriers on heating that triggers the Maxwell-Wagner relaxation that results in the $\epsilon' = 6000$ plateau in Figs. 2 and 3.

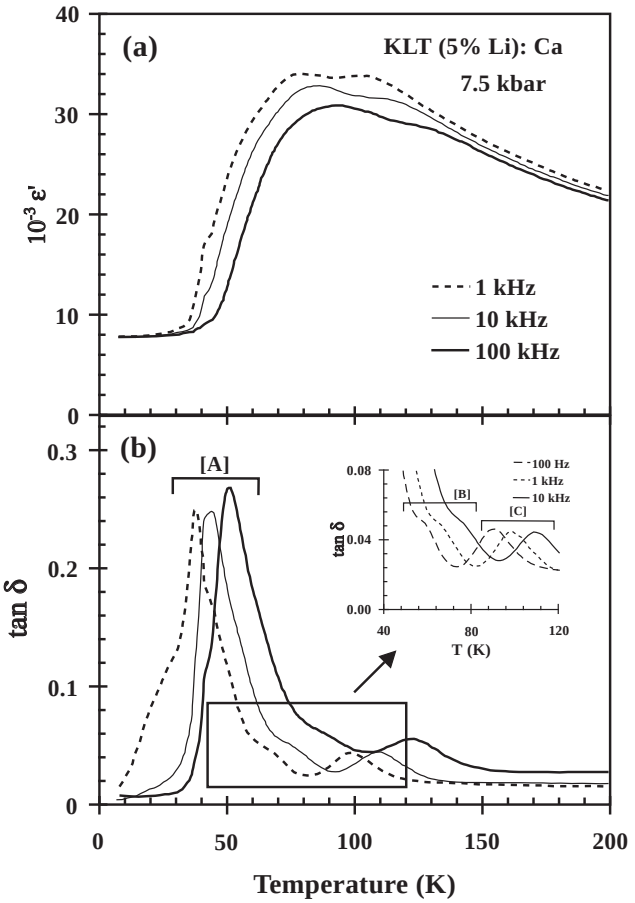

FIG. 5: The dielectric $\epsilon'(T)$ and $\tan\delta$ responses of KLT(5):Ca at 7.5 kbar. Pressure shifts the responses to lower Ts and sharpens the relaxational features (compare to Fig. 2).

increase in the conductivity. It is this increase in sample conductivity that is responsible for the increase in the amplitude of $\epsilon'(T)$ in the plateau region with pressure. Simply stated, the higher the conductivity of the sample, the greater is the conductivity mismatch at the barrier layer and the higher is the relaxation step in ϵ'.[20]

A similarity between the results shown in Fig. 2 (a) for KLT(5):Ca and the undoped KLT(4.3) in the inset is represented by the shape of the $\epsilon'(T)$ response with its overlapping peaks, despite the fact that the absolute amplitudes of $\epsilon'(T)$ for the two materials are vastly different. In fact, the response in Fig. 2 (a) is qualitatively like that of undoped KLT(5), but "sitting on top of" an $\epsilon' \sim 6000$ baseline. Remarkably, for the undoped crystal in the inset, ϵ'_{max} at the relaxational peak is $\sim 6\times$ its value at low temperatures, and this ratio is about the same for the KLT(5):Ca crystal. Pressure shifts the $\epsilon'(\omega, T)$ response to lower temperatures and sharpens it somewhat maintaining its relaxor character (Fig. 5).

An additional feature in the $\epsilon'(T)$ response in Fig. 2 (a) is the structure at temperatures below ϵ'_{max}. This structure is revealed more distinctly in the $\tan\delta(\omega, T)$ response illustrated in Figs. 2 (b) and 5 (b). Some of this response is probably due to some inhomogeneities or defects in the crystal, but there are three sets of relaxational peaks that we wish to draw attention to. These are labeled A, B and C in Figs. 2 (b) and 5 (b) and all are Debye-like, the relaxational frequency (or inverse relaxation time, τ) obeying Arrhenius kinetics

$$\omega = \tau^{-1} = \omega_o \exp(-E/kT) \qquad (1)$$

as shown for A and C in Fig. 6. The kinetic parameters are: $E = 79(244)$ meV and $\omega_o = 4.2 \times 10^{12}(5 \times 10^{15})$ s^{-1} for A (C), respectively. These parameters are in close agreement with the above-cited values for the reorientation of the isolated Li^+ and Li^+-Li^+ ion pair dipoles, respectively, in undoped KLT, and, thus, are unaffected by the light Ca doping.

The mechanism for the reorientation of the Li^+ dipole is by $\pi/2$ (90°) flips of the dipolar orientation among the six equivalent Li sites (Fig. 1 (b)).[18,19,22] At the 5 % Li concentration in KLT(5):Ca, the Li^+ - Li^+ ion pairs signature is clearly present in both the ϵ' and $\tan\delta$ data. The reorientation of this ion pair is believed to be associated with the reorientation of two nearest-neighbor Li^+ ions.[18,19,21,22,23] Doussineau *et al.*[18] have suggested that, in their two degenerate lowest energy configurations, the

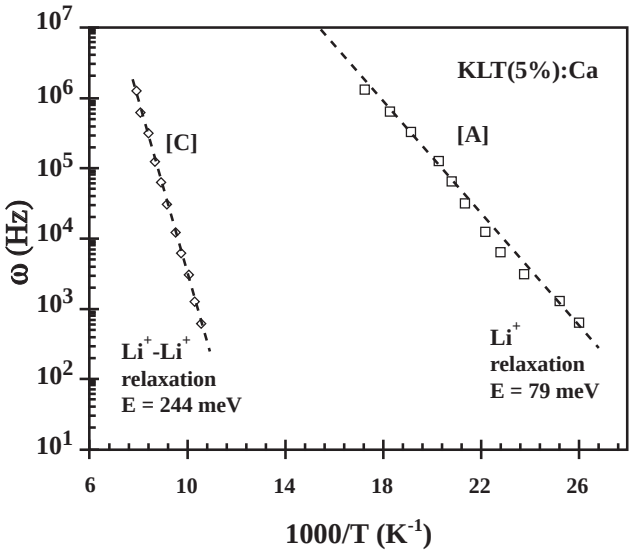

FIG. 6: Arrhenius plots for the Li^+ [A] and Li^+-Li^+ pair [C] dipolar relaxations in KLT(5):Ca at 1 bar.

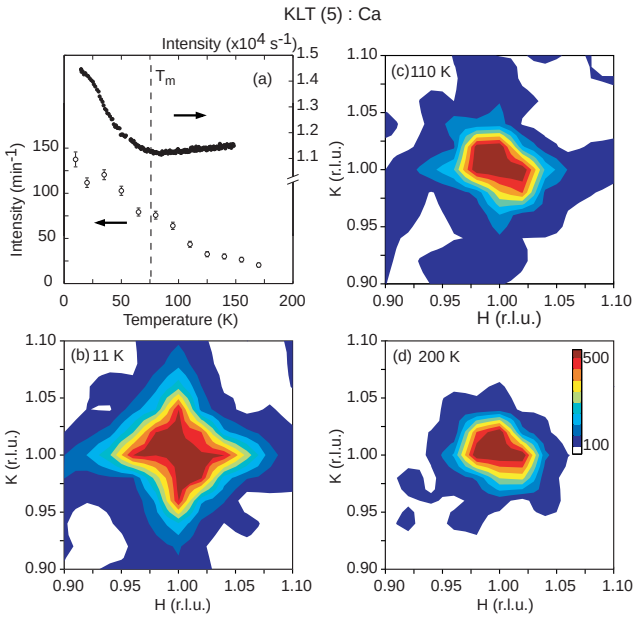

FIG. 7: (Color online) (a) Temperature dependence of the $(2,0,0)$ nuclear Bragg peak (black circles) and the diffuse scattering intensity measured at $(1.05,1,0)$. (b)-(d) Contour maps of the diffuse intensity around $(1,1,0)$ at 11 K, 110 K, and 200 K.

pair dipoles are collinear and aligned parallel to the line that joins their sites. The relaxation mechanism involves a simultaneous reversal of both dipoles in π (180°) flips [Fig. 1 (c)]. Support for this mechanism comes from the absence of this relaxation in ultrasonic measurements.[18,22] Because the postulated Li^+ - Li^+ pairs are centro-symmetric, a flip leaves the quadrupole moment invariant, and this relaxation mode is not coupled to acoustic waves. Support has also come from recent first-principles calculations on KLT supercells.[23] These calculations indicate that the pairs 180° reorientation proceeds via metastable intermediate steps. Additionally, the calculated hopping barriers for both the isolated Li^+ dipole and the pair are found to be in reasonable agreement with those deduced from the dielectric measurements.

Relaxation B appears as a peak in $\tan\delta$ at 100 Hz, but is a shoulder at other frequencies. This shoulder becomes more prominent and more separated from the A and C relaxations at high pressure [Fig. 5 (b)]. An approximate separation of the B peaks, shows that this relaxation is also Debye-like with the same activation energy $E \sim 135$ meV. We attribute this new B relaxation in KLT(5):Ca to the Ca^{2+} dopant, since it is not observed in undoped KLT. But in any case, it is a minor feature in the response of KLT(5):Ca.

B. Diffuse scattering and atomic shifts

In the prototypical relaxor like $Pb(Mg_{1/3}Nb_{2/3})O_3$ (PMN), it is well established that diffuse neutron scattering appears around the nuclear Bragg peaks below the so-called Burns temperature - below which the polar nano-regions (PNR's) appear.[7] Therefore, the diffuse scattering originates from the atomic displacements in PNR's, and its structure factor $F_{diff}(\mathbf{Q})$ can be written as

$$F_{diff}(\mathbf{Q}) = \sum_{\kappa}[\mathbf{Q}\cdot\vec{\delta}_{\kappa}]b_{\kappa}e^{i\mathbf{Q}\cdot\mathbf{d}_{\kappa}}e^{-W_{\kappa}}, \qquad (2)$$

where $\vec{\delta}_{\kappa}$, b_{κ}, $\mathbf{d}_{\kappa}$, and $e^{-W_{\kappa}}$ are the atomic shift, neutron scattering length, coordination vector, and Debye-Waller factor (approximately 1) for κ atoms, respectively. Note that the diffuse scattering intensity is proportional to $|F_{diff}|^2$. For PMN, anomalous atomic shifts in the PNR's are reported; the total shift is composed of two components - one is a set of shifts that conserves the center-of-mass (CM) condition, and the other is a uniform phase shift.[9] To verify if such anomalous shifts are also realized in the KLT system, we have carried out a study of the diffuse scattering from KLT(5):Ca.

The black circles in Fig. 7 (a) show the temperature dependence of the (200) nuclear Bragg peak. Some relaxors that have an actual FE transition at T_c, such as KLT with higher Li concentration and $Pb(Zn_{1/3}Nb_{2/3})O_3$ (PZN) have been reported to show an increase in the nuclear Bragg peaks below T_c due to a release of extinction. The present KLT(5):Ca crystal shows an increase of the (200) intensity below 75 K. Although our crystal does not show a sharp peak in the dielectric response at 75 K, this temperature is consistent with the first hump in the $\epsilon'(T)$ response in Fig. 2 (a) that corresponds to the slowing down of the fluctuations of the Li^+ dipoles. Additionally, the increase of the nuclear Bragg intensity

in the present crystal is only ~ 50 % and it occurs gradually with decreasing temperature. This is in contrast to the behavior of KLT crystals with higher Li content which have a well-defined FE transition in the dielectric measurements; for these latter crystals the nuclear peak intensity increases rapidly by more than an order of magnitude at T_c.[6,24] These facts suggest that the present crystal has a very small volume fraction of any ferroelectrically transformed area, and that a relaxor state is still dominant below 75 K, a conclusion supported by the dielectric results. Hereafter, we define this temperature as T_m (not T_c) since no bulk FE transition occurs in our crystal.

Temperature variations of the diffuse scattering around the (110) position are shown in Figs. 7(b) - 7(d). At $T = 11$ K, diffuse scattering ridges along the H and K directions are clearly observed. At $T = 110$ K, which is ~ 35 K higher than T_m, the diffuse ridges are still visible, and then, the diffuse scattering finally becomes unobservable at 200 K. The temperature dependence of this scattering intensity measured at $(1.05, 1, 0)$ is indicated in Fig. 7 (a) by open circles and shows gradual increase starting at ~ 150 K, suggesting that the Burns temperature of this system should be above this temperature. The diffuse scattering does not show the critical scattering behavior around T_m, that is observed in relaxor materials with a well-defined T_c, such as PZN[25] and KLT with higher Li content.[6] Again, this is supporting evidence that the present sample does not have a ferroelectrically well-ordered state.

The observed diffuse scattering ridge along the [100] direction in the reciprocal space should correspond to a disk shape of PNR's which spreads in the {100} plane in the real space, as discussed in Ref. 6. Similar *pancake* shaped PNR's in PMN and PZN-PT have been discussed in Ref. 26. From the width of the diffuse peaks, we estimate the dimensions of the disk PNR's as 52(±10) Å in the {100} plane and 16(±3) Å thickness in the [100] direction.

Diffuse scattering profiles at several zones are shown in Fig. 8. A clear diffuse component appears as wide intensity tails around (110), and a small diffuse intensity is observed around (210). For (200), the longitudinal profile (H-scan) is somewhat peculiar; the Bragg peak itself has already a wide tail even at 160 K. (We note that a small hump at $H = 1.93$ is a powder line from the aluminum surrounding the sample.) The presence of this tail at this high temperature may be related to the dielectric results in Fig. 2 (a) that show relaxation associated with the Li^+-Li^+ dipolar pairs that extends to ~ 200 K. We also find that there is an intensity difference between the results obtained at 160 K and 10 K at $H \sim 2.05$. This difference, however, is suppressed quickly at $H = 2.07$, whereas the diffuse scattering decays gradually up to $q = 0.1$. Therefore, we conclude that the difference in intensities at $H = 2.05$ is not associated with diffuse scattering but results from possible broadening of the Bragg peak in the longitudinal direction below T_m.

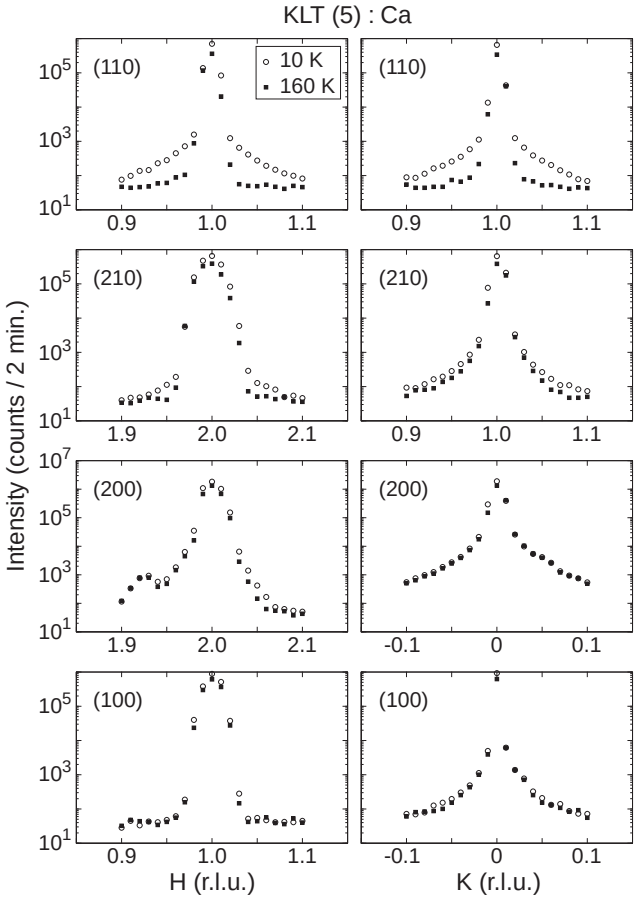

FIG. 8: Comparison of diffuse scattering peaks at 10 K (open circles) and at 160 K (black circles) at various **Q** positions. Left and right figures show scans along the H and K directions, respectively.

Apparently, there is no clear diffuse signature around (100). Based on Eq. 2, structure factors for both (100) and (210) can be written as $F_{diff}(\mathbf{Q}) = [\mathbf{Q}\cdot\hat{\delta}](A-B-O)$ where $A = 0.95\delta_{\rm K}b_{\rm K}+0.05\delta_{\rm Li}b_{\rm Li}$, $B = \delta_{\rm Ta}b_{\rm Ta}$, $O = \delta_{\rm O}b_{\rm O}$, and $\hat{\delta}$ is a unit vector. This means that the difference in the diffuse intensity between (100) and (210) arises from $|\mathbf{Q}|^2$. Our observation demonstrates an existence of diffuse intensity at (210), thus, the diffuse intensity at (100) should be simply too small to observe rather than being zero.

In order to derive the atomic shifts by using Eq. 2, we employ the relation $F_{diff}(110) = 1.93F_{diff}(210)$ and $F_{diff}(200) = 0$. The former is based on a comparison of the diffuse intensities at $(1.05, 1, 0)$ and $(2.05, 1, 0)$. Then we assume $\hat{\delta}$ to be parallel to the Li off-center direction, either [100] or [010]. Thus the local crystal symmetry inside the PNR is tetragonal. The PNR's with $\hat{\delta} = [100]$ and [010] are also assumed to be distributed with same population. These conditions give $A = -1.66O$ and $B = -1.34O$. Here we use the quantities $b_{\rm K} = 0.35$, $b_{\rm Ta} = 0.70$, and $b_{\rm O} = 0.58$, and, for simplicity, neglect the $\delta_{\rm Li}$

contribution since the Li content (5 %) is relatively low. Then atomic shifts that are normalized to the shift of the oxygen atom ($\delta_{\rm O}$) are obtained as

$$\begin{aligned}\delta_{\rm K} &= -2.89,\\ \delta_{\rm Ta} &= -1.11,\\ \delta_{\rm O} &= 1.00.\end{aligned}$$

Remarkably, these values do not satisfy the CM condition, $\sum_\kappa \delta_\kappa M_\kappa = 0$, where M is an atomic mass, $M_{\rm K} = 39$, $M_{\rm Ta} = 181$, and $M_{\rm O} = 16$. A similar breaking of the CM rule has been found in the atomic shifts of PMN.[8] Hirota *et al.*[9] proposed a model of TO phonon condensation with a uniform phase shift. In this model, the atomic shift can be expressed as $\delta_\kappa = \delta_\kappa^{cm} + \delta_\kappa^{us}$, where δ_κ^{cm} originates from the condensation of the TO soft mode conserving the CM condition, whereas δ^{us} is a uniform shift of PNR's relative to the surrounding cubic matrix. Following the same procedure employed by Hirota *et al.*, we obtain

$$\begin{aligned}\delta_{\rm K}^{cm} &= -1.90,\\ \delta_{\rm Ta}^{cm} &= -0.12,\\ \delta_{\rm O}^{cm} &= 1.99,\\ \delta^{us} &= -0.99.\end{aligned}$$

It should be noted that, once the diffuse intensity ratios at different zones are given, the above quantities δ, δ^{cm}, and δ^{us} are uniquely derived only by a mathematical procedure. The validity of the model can be tested by checking to see if δ^{cm} can reproduce the intensity ratio of the zone center TO mode. If δ_κ^{cm} originates from the condensation of the TO soft mode, it should be proportional to the phonon polarization vector $\vec{\xi}_\kappa$. The inelastic structure factor $F_{inel}(\mathbf{Q})$ is expressed basically by the same formula as Eq. 2 where $\vec{\delta}_\kappa$ should be replaced by $\vec{\xi}_\kappa$. From the obtained $\delta_\kappa^{cm}(\propto \xi_\kappa)$, a ratio of the inelastic structure factors $|F_{inel}(200)|/|F_{inel}(110)|$ is calculated to be ~ 2.9. The observed zone-center TO phonons at (200) and (110) are shown in Fig. 9 which were measured at room temperature. The solid lines are fits to a Lorentzian phonon crosssection and a Gaussian peak at energy transfer $\Omega = 0$ convoluted with an instrumental resolution function. (The actual formula is given in the next section.) Our fits give $|F_{inel}(200)|/|F_{inel}(110)| = 3.3(\pm 0.3)$, which is in agreement with the value calculated from δ^{cm}.

Another check of the consistency of the data may be achieved by determining the contributions of the Slater and Last modes, which are two dominant optic modes in perovskite materials. In case of KLT, the Slater mode corresponds to an atomic motion whereby the oxygen ions and Ta ions move in opposite directions while the K ions do not move. The Last mode corresponds to the counter displacements of the TaO_6 octahedra and K ions. In order to satisfy the CM condition, the amplitudes $(\xi_{\rm K}, \xi_{\rm Ta}, \xi_{\rm O})$ for the Slater and Last modes should be $\vec{s}_1 = (0, -0.265, 1)$ and $\vec{s}_2 = (-5.872, 1, 1)$, respectively. Designating the contributions of the Slater and Last modes to S_1 and S_2, respectively, we obtain $S_1\vec{s}_1 + S_2\vec{s}_2 = (\xi_{\rm K}, \xi_{\rm Ta}, \xi_{\rm O})$, giving $S_1 \sim 1.6$ and $S_2 \sim 0.3$. Harada *et al.*[27] have reported an almost 100 % contribution of the Slater mode in the non-Li-doped KT, which is qualitatively consistent with the present observation giving an 85 % contribution by the Slater mode. In the Li-doped samples, it is possible that the K-ions can move more since the doped Li ions with their smaller radius effectively provide more space. This is possibly why we have a somewhat larger contribution of the Last mode in KLT than in KT. (In the same mannar, the small amount of Ca ions in our crystal, which shift to the off-center positions in combination with the oxygen vacancies, may also cause the same effect.)

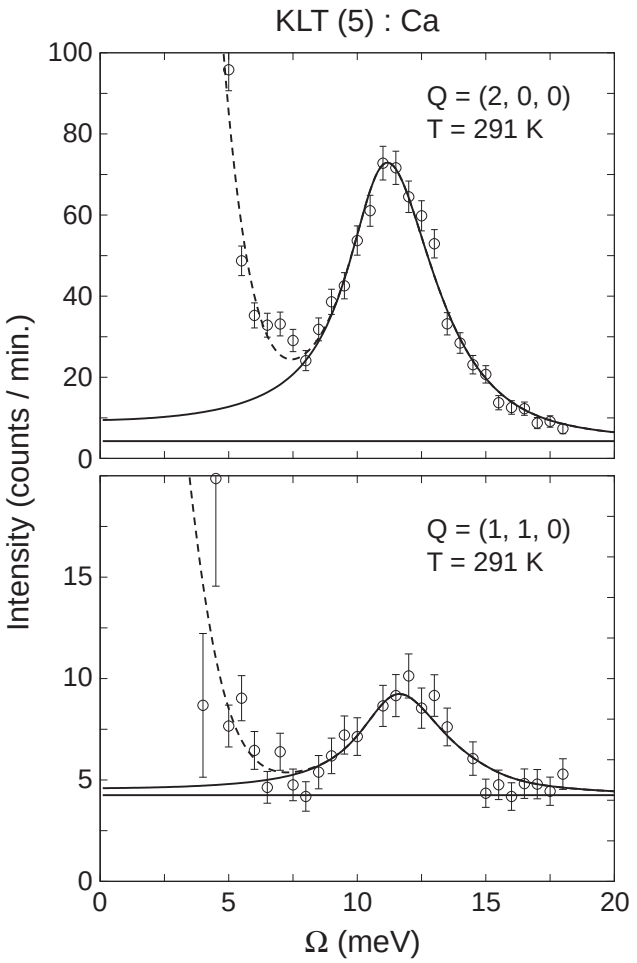

FIG. 9: Zone center optic phonon profiles at $(2,0,0)$ (top) and $(1,1,0)$ (bottom). Solid lines are fits to a resolution-convoluted Lorentzian function, while the dashed lines represent a Gaussian peak component at $\Omega = 0$.

The diffuse scattering in the relaxor KLT(5):Ca, therefore, exhibits analogous behavior to that of the prototypical relaxor PMN. Remarkably, the atomic shifts in KLT, that are characterized by the diffuse intensities, can be consistently explained by the uniform phase shift model introduced by Hirota *et al.* Accordingly, it is likely that

the uniform phase shift is a common feature in relaxor systems and is a key to understanding the fundamentals of the relaxor mechanism.

The origin of the uniform phase shift remains somewhat of an open question. Hirota *et al.*[9] have hypothesized that the phase shift in PMN occurs as the polarized regions slide on an electric field gradient which is due to the existence of chemical ordered and disordered domains. In the ordered domain, Mg^{5+} and Nb^{2+} ions are ordered in 1:1 ratio, which breaks the charge neutrality in the domains, and thence the electric field gradient is induced in a comparable length scale to the PNRs. Although there are no such the electric field gradient in KLT, as Li^{+} and K^{+} have the same valence, a somewhat analogous mechanism is likely operable. In this case, the large off-center displacements of Li ions produce two dipolar entities that are sources of random electric fields that can trigger the phase shift. Thus, we envision that for both KLT and PMN electric fields trigger the phase shift which is then superimposed on the ionic displacements associated with the FE soft mode resulting in the total measured displacements within the PNRs.

C. Lattice dynamics

In relaxor materials, anomalies of the transverse optic (TO) and the transverse acoustic (TA) phonons are expected to accompany PNR formation. A feature that has recently attracted a significant amount of attention is the strong damping of the TO mode below the Burns temperature at small q, a feature observed in both PZN[28] and PMN[29]. This is interpreted as a result of PNR formation that disrupts the long wave-length, i.e. small-q, optic mode. Also, the line width of the TA mode has been found to broaden below the Burns temperature.[30] We have studied the TA and TO phonons in the present relaxor KLT(5):Ca crystal in order to understand the lattice dynamics and to learn if such phonon anomalies are universal features of relaxors. It should be noted that the TO phonon in KLT originates mostly from the dynamics of the TaO_6 octahedra since the Slater mode is highly dominant as mentioned earlier. On the other hand, the relaxational behavior of doped Li ions appears in the dielectric response as we see in Sec. IV A.

We have measured the phonons around the (200) Bragg peak since phonon structure factors at the other Q positions that are accessible in the present condition of $E_f = 14.7$ meV are quite small. Figure 10 shows representative profiles of the TO phonons at the zone center (200) and of the TA phonons at $(2, -0.15, 0)$. It is seen that, with decreasing temperature, the phonon energy of the zone-center TO mode decreases and the line width apparently increases, but the phonon remains a well-defined excitation at all temperatures. The TA phonon peak also broadens as the temperature decreases.

In order to extract more insight, all of the profiles have

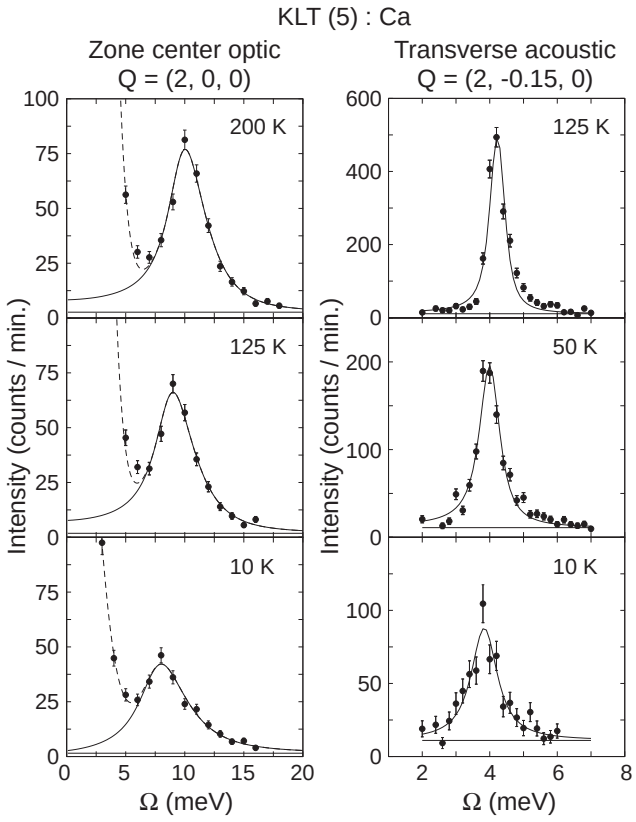

FIG. 10: Zone center TO phonon measured at $(2, 0, 0)$ (left figures) and the TA phonon measured at $(2, -0.15, 0)$ (right figures). Solid lines are fits to a resolution-convoluted Lorentzian function.

been analyzed by fitting to the resolution-convoluted phonon scattering function

$$S(\mathbf{q}, \Omega) = [n(\Omega) + 1]\chi''(\mathbf{q}, \Omega), \tag{3}$$

$$\chi''(\mathbf{q}, \Omega) = \frac{I}{(\Omega - \Omega_{ph}(\mathbf{q}))^2 + \Gamma(\Omega)} - \frac{I}{(\Omega + \Omega_{ph}(\mathbf{q}))^2 + \Gamma(\Omega)}, \tag{4}$$

where Ω is the neutron energy transfer $E_i - E_f$, $n(\Omega) = 1/(e^{\Omega/k_BT} - 1)$ is the Bose factor, Ω_{ph} is the phonon energy, $\Gamma(\Omega)$ is the half-width-at-half-maximum (HWHM) of the phonon spectrum, and I is the amplitude. To fit the TO spectra, the following dispersion relation was utilized;

$$\Omega_{ph}^2(q) = \Omega_0^2 + (Cq)^2, \tag{5}$$

where Ω_0 is a zone-center TO phonon energy, and $C = 40.3$ meV^{2}Å^2 determined from the dispersion at room temperature. For fitting of the TA profiles, the dispersion is taken to be linear in q.

The fits thus obtained are shown by solid lines in Fig. 10 where the flat background is also adjusted. Dashed lines represent elastic peaks at $\Omega = 0$ which are assumed to be Gaussians. The fitting parameters are summarized

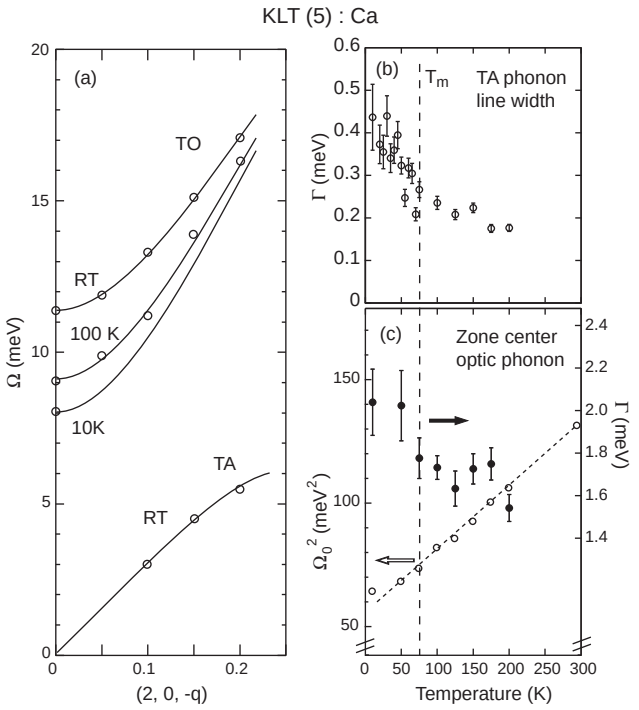

FIG. 11: (a) Dispersions of the TO and TA phonons measured in the $(2, 0, 0)$ zone. (b) Temperature dependence of the line width Γ of the TA phonon measured at $(2, -0.15, 0)$. (c) Zone-center TO phonon energy squared Ω_0^2 (open circles) and phonon line width Γ (black circles) as a function of temperature.

in Fig. 11. As shown in Fig. 11 (a), the TO mode softens gradually with decreasing temperature, but the dispersion is well-defined at all temperatures - in contrast to those of PMN and PZN. The TO mode softening is clearly seen in Fig. 11 (c) where the zone-center TO phonon energy squared Ω_0^2 plotted by open circles decreases linearly with temperature. This implies that the system still maintains an incipient lattice instability towards the ferroelectric state even with dopant Li ions present, similar to KT[2] and several KLT compositions.[4] Although the TO dispersion is well-defined at all temperatures, the TO phonon peak shows a small broadening at low temperatures. The line width Γ of the TO mode at the zone center, represented by the closed symbols in Fig. 11 (c), increases with decreasing temperature, characteristic soft mode behavior for ABO_3 perovskites.

The TA phonon dispersion at room temperature is shown in Fig. 11 (a). We have observed a small softening by ~ 1 meV of the TA phonon energy at $q = 0.15$ r.l.u. from room temperature to 10 K with a linear decrease in this energy. The TA phonon peaks are sharp and nearly resolution limited. It is somewhat difficult to evaluate an intrinsic line width by deconvolution analysis which gives a large ambiguity for the resolution-limited peaks. Therefore, we have fit the TA profiles to a simple Lorentzian function to determine an effective line width. The line width, shown in Fig. 11 (b), increases with decreasing temperature even above T_m. This temperature-dependence resembles that of the diffuse intensity shown in Fig. 7 (a), implying that the TA line broadening accompanies the formation of PNR's.

There are interesting similarities and differences in the phonon behavior between the present KLT(5):Ca material and the prototypical relaxors PMN and PZN. In the case of PMN and PZN, the TO phonon softens following $\Omega_0^2 \propto T$ above the Burns temperature T_d. It then becomes strongly damped in the temperature range of T_c(or T_m) $< T < T_d$, and finally recovers below T_c (T_m) - and subsequently hardens with further decrease in T - again following $\Omega_0^2 \propto T$.[25,30] For the present KLT(5):Ca crystal, the TO phonon softens in the same manner, although it does not harden below T_m because there is no macroscopically well-developed ferroelectric state. The softening at high temperatures for all these materials means that the relaxor state sets in ABO_3 lattices that have incipient lattice tendencies towards ferroelectric transitions. This is as expected because the high polarizability of these FE mode lattices results in large correlation lengths for dipolar interactions and favors the formation and growth of PNR's below the Burns temperature.[20] No hardening of the TO phonon below T_m in the present crystal means that the sample remains in the relaxor state at low temperatures. Consistent with this conclusion, the crystal shows neither a well-defined transition in the dielectric measurements nor a large extinction release of the nuclear Bragg peaks.

Another observed difference between KLT and PMN (PZN) is the absence of strong damping of the TO phonon in the present KLT(5):Ca crystal, which is frequently associated with the "waterfall" anomaly observed in PMN and PZN. We speculate that this absence of strong damping occurs because the PNR's in the KLT(5):Ca crystal have small size and a small volume fraction. Thus, these PNR's are not robust enough to dampen the TO phonon, but nevertheless can broaden the line width as shown in Fig. 11 (c). An alternative explanation for the waterfall effect has come from a recent neutron scattering study of 60%-$PbTiO_3$ doped PMN by Stock *et al.*[35] that revealed the existence of the waterfall anomaly even though the sample exhibits long-range order, suggesting that the waterfall is unrelated to PNR's. They have argued that the waterfall results from random fields due to the chemical disorder (i.e., valence fluctuations). It is important to note, however, that although mixed $PbTiO_3$-PMN samples exhibit FE order, they are highly, compositionally disordered and still exhibit considerable relaxor character. If random fields are responsible for the waterfall effect, then it should be seen in KLT where the Li dipoles produce strong random fields. Therefore our conclusion at this time is that the PNR explanation for the waterfall effect should not be dismissed. However, further work is necessary to firm up the origin of this interesting effect.

As for the TA phonon behavior, in contrast to our

KLT(5):Ca sample, Toulouse and Hennion[31] have reported that the TA phonon of KLT(3.5) splits into two modes below $T_c = 52$ K corresponding to a tetragonal symmetry of the ferroelectric state. (They claim that their KLT(3.5) sample shows an FE transition at 52 K from the dielectric measurements.[31]) Our crystal shows only TA phonon broadening and no splitting because it does not have a ferroelectric transition. As shown in Fig. 11 (b), the TA broadening appears to start above T_m, and possibly at T_d which should be around 200 K as noted earlier based on the dielectric measurements and the diffuse scattering. Thus, the TA phonon is also affected by PNR formation. In contrast to this behavior, PMN and PZN have been reported to show TA phonon broadening at temperatures in the range of $T_c < T < T_d$.[30] Such behavior has been recently interpreted in the framework of a coupling of the TA mode to the diffuse component since the TA broadening is strong at the **Q** positions where the diffuse scattering is strong.[32,33] More detailed measurements are necessary to determine if such coupling effects also exist in KLT as a manifestation of a common feature of relaxors.

Finally we discuss the TO phonon energy that depends on the Li concentration. Comprehensive study of the TO soft mode using hyper-Raman spectroscopy for various Li concentrations have been carried out by Vogt.[4] It is clearly demonstrated that the TO mode frequency Ω_0 increases with Li content x following a linear relation

$$\Omega_0^2(x,T) = \Omega_0^2(0,T) + Ax. \qquad (6)$$

In fact, the Ω_0 value of our KLT(5):Ca crystal is higher than that of the pure KT measured by the neutron scattering by Axe *et al.*[2] However, it is even higher than that of the $x = 0.087$ sample measured by Raman spectroscopy by Vogt. To address this problem, we test the relation of Eq. 6 using the present KLT(5):Ca sample and another KLT crystal with $x = 0.10$.

The latter sample was grown in the same manner, but is free from Ca impurity. It has a clear FE transition at $T_c = 113$ K evidenced from dielectric measurements and neutron scattering experiments. (Details of this sample will be published elsewhere.[24]) The quantities of $T_m = 75$ K for KLT(5):Ca and $T_c = 113$ K for KLT(10) are consistent with *freezing temperatures*, T_g, summarized in Ref. 34, suggesting a validity of the estimation of the Li contents.

The zone-center TO phonon energy squared $\Omega_0^2(x,T)$ at $T = 10$ K and 300 K are shown in Fig. 12, together with those of pure KT referred from Ref. 2. It is clearly demonstrated that the linear relation of Eq. 6 stands for the series of our samples. This is further evidence of proper Li concentrations of our samples, and also, it implies that the small amount of Ca impurity has only a minor effect on the lattice dynamics properties. We believe that the disagreement of Ω_0 with those of Raman data by Vogt is due to a systematic difference of the Li content evaluation.

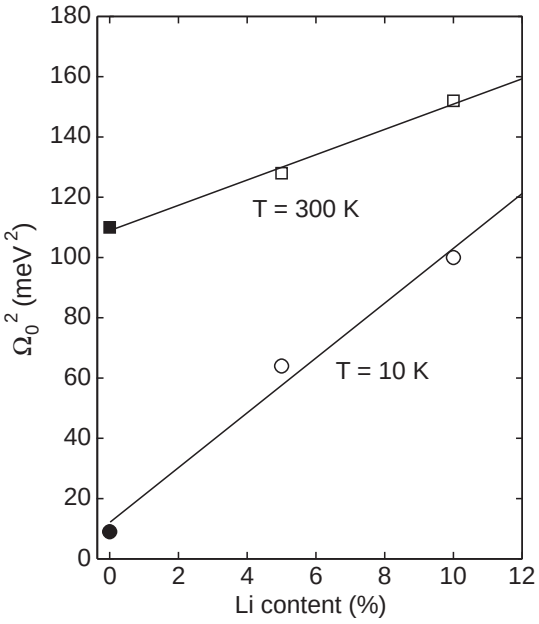

FIG. 12: Li concentration dependence of Ω_0^2 at $T = 10$ K and 300 K. Data of pure KT (closed symbols) are adopted from Ref. 2. The lines are results of fits to Eq. 6.

V. CONCLUDING REMARKS

The origins of some aspects of the relaxor behavior in ABO_3 oxides remain as somewhat open questions. For the prototypical relaxors PMN and PZN, however, it is clear that the chemical (valence) disorder of the Mg and Nb ions and the associated random fields play an important role by disrupting FE correlations leading to the relaxor state. In the KLT system Li dipoles also produce random fields that are thought by some to be responsible for the relaxor behavior (e.g., see Ref. 36). We note, however, that the situation in KLT is different from that in most ABO_3 relaxors in that the parent crystal KT has no FE order to disrupt. In fact, at very low Li concentration in KT the Li dipoles exhibit essentially dipolar glass response with no correlations among dipoles. Such correlations develop with increasing Li concentration leading to the evolution of a relaxor state

Combining the relaxational behavior and the neutron scattering results, we can draw the following picture for KLT(5). At the Burns temperature, PNR's start to form triggered by off-center displacements of the Li ions. The symmetry of these polar regions is tetragonal, and the observed ionic displacements consist of the displacements associated with the soft FE mode on which is superimposed a uniform phase shift.

Below the Burns temperature, the dynamics of Li atoms appears as the relaxational behavior in the dielectric response. As temperature decreases dipolar fluctuations are reduced and stronger correlations develop among the PNRs that grow in volume, as evidenced by the growth of diffuse scattering intensity. Slowing down

of dipolar fluctuations sets in at a temperature corresponding to the peak temperature in the dielectric constant and continues on further cooling. Although the present sample shows no bulk FE transition, the increase of the Bragg intensity below ~ 75 K, where the Li-Li pair becomes well static ($1000/T \sim 13$ in Fig. 6) is indicative of larger PNRs (which are nano FE domains) or even the presence of larger FE domains in a sea of relaxor phase.

In summary, we have measured the dielectric response and lattice dynamics in the relaxor KLT(5):Ca where a small amount of Ca was incorporated into the KLT crystal. Both types of results affirm that the present crystal remains in the relaxor state and does not develop a ferroelectric state at low temperatures. Dielectric constants that are sensitive to impurities exhibit strong enhancement attributed to free electrons from the Ca dopant, however the relaxational features including Arrhenius parameters of Li^+ ion and Li^+-Li^+ pair dipolar relaxations are not affected by the Ca.

Neutron scattering results for KLT(5):Ca compared with those of the relaxor PMN highlight common features in relaxors. Lattice displacements in PNR's derived from the diffuse intensities suggest that the model of the normal soft-mode condensation with an additional uniform phase shift within the PNR's is also relevant in KLT. This means that we cannot rule out a contribution of the zone-center TO soft mode to the formation of PNR's. However, the TO soft mode remains at relatively high energy compared to that of PMN, and it also remains well-defined in contrast to the heavily-damped nature characteristic of PMN. We believe that this difference reflects the fact that KLT(5):Ca is a weak relaxor, essentially a dipolar glass, whereas PMN is the prototypical strong relaxor. A more comprehensive study will be required in order to extract the precise nature of the specific coupling between the TO phonon and the relaxor mechanism in this system.

Acknowledgments

The authors thank B. Burton, T. Egami, R. Erwin, P. M. Gehring, K. Hirota, K. Kakurai, and N. Metoki for invaluable discussions. This work was partially supported by the US-Japan Cooperative Research Program on Neutron Scattering. Work at Sandia National Laboratory was supported by the Division of Material Sciences and Engineering, Office of Basic Energy Sciences, U.S. Department of Energy under Contract DE-AC04-94AL85000. Research sponsored in part by the Division of Material Sciences and Engineering, Office of Basic Energy Sciences, U.S. Department of Energy under Contract DE-AC05-00OR22725 with Oak Ridge National Laboratory, managed and operated by UT-Battelle, LLC. Finally, work at Brookhaven National Laboratory is supported by financial support from the U. S. Department of Energy under Contract No. DE-AC02-98CH10886.

* Corresponding author: wakimoto.shuichi@jaea.go.jp

[1] S. H. Wemple, Phys. Rev. **137**, A1575 (1964).
[2] J. D. Axe, J. Harada, and G. Shirane, Phys. Rev. B **1**, 1227 (1970).
[3] P. Calvi, P. Camagni, E. Giulotto, and L. Rollandi, Phys. Rev. B **53**, 5240 (1996).
[4] H. Vogt, J. Phys:Cond. Matter **7**, 5913 (1995); Ferroelectrics **184**, 31 (1996); **202**, 157 (1997).
[5] R. L. Prater, L.L. Chase and L. A. Boatner, Phys. Rev. B **23**, 5904 (1981).
[6] G. Yong, J. Toulouse, R. Erwin, S. M. Shapiro, and B. Hennion, Phys. Rev. B **62**, 14736 (2000).
[7] A. Naberezhnov, S. Vakhrushev, B. Doner, D. Strauch, and H. Moudden Eur. Phys. J. B **11**, 13 (1999)
[8] S. B. Vakhrushev, A. A. Naberezhnov, N. M. Okuneva, and B. N. Savenko, Fiz. Tverd. Tela (St. Petersburg) **37**, 3621 (1995) [Phys. Solid State **37** 1993 (1995)].
[9] K. Hirota, Z.-G. Ye, S. Wakimoto, P. M. Gehring, and G. Shirane, Phys. Rev. B **65**, 104105 (2002).
[10] We have performed inductively coupled plazma (ICP) analysis on the starting powder materials. The following metals were sought: Ca, Bi, Cr, Fe, Mn, Sr, V. Sb, B, Co, Pb, Mo, Si, Te, Zn, As, Cd, Cu, Ni, Ag, Sn, Zr, Ba, In, Mg, P, Na, and Ti. The ICP analytical results did reveal the presence of $<$ 15 ppm of only Ca in the potassium carbonate.
[11] J. J. van der Klink and F. Borsa, Phys. Rev. B **30**, 52 (1984).
[12] G. A. Samara in Solid State Physics, Vol.56 edited by H. Ehrenreich and F. Spaepen, Academic Press, New York (2001) p. 239 and references therein.
[13] U. T. Hochli, K. Knorr and A. Loidl, Adv. Phys. **39**, 405 (1990).
[14] Y. Yacoby and S. Just, Solid State Commun. **12**, 715 (1974).
[15] K. Leung, Phys. Rev. B **65**, 012102 (2001).
[16] L.S. Senhouse, Jr., M.V. DePaolis, Jr. and T.L. Loomis, Appl. Phys. Lett. **8**, 173 (1966).
[17] S. A. Prosandeev, V.A. Trepakov, M.E. Savinov, J. Jastradik and S.E. Kapphan, J. Phys.: Condens. Matter **13**, 9749 (2001).
[18] P. Doussineau, Y. Farssi, C. Frenos, A. Levelut, K. McEnaneu, J. Toulouse and S. Ziolkiewicz, Europhys. Lett. **24**, 415 (1993).
[19] J. Toulouse and R. Pattnaik, J. Korean Phys. Soc. **32**, S942 (1998).
[20] R. K. Grubbs, E. L. Venturini, P. G. Clem, J. J. Richardson, B.A. Tuttle and G. A. Samara, Phys. Rev. B **72**, 104111 (2005). See also J. Volger in *Progress in Semiconductors*, edited by A. F. Gibson (John Wiley and Sons, New York 1960), vol. 4, p. 207.
[21] S. H. Wemple, M. DiDomenico, Jr. and A. Jayaraman,

Phys. Rev. **180**, 547 (1969).
[22] H. M. Christen, U.T. Hochli, A. Chatelain and S. Ziolkiewicz, J. Phys.: Condens. Matter **3**, 8387 (1991).
[23] S.A. Prosandeev, E. Cockayne and B.P. Burton, Phys. Rev. B **68**, 014120 (2003).
[24] S. Wakimoto, G. A. Samara, and L. A. Boatner, unpublished.
[25] C. Stock, R.J. Birgeneau, S. Wakimoto, J.S. Gardner, W. Chen, Z.-G. Ye, and G. Shirane, Phys. Rev. B **69**, 094104 (2004).
[26] G. Xu, Z. Zhong, H. Hiraka, and G. Shirane, Phys. Rev. B **70**, 174109 (2004).
[27] J. Harada, J. D. Axe, and G. Shirane, Acta Cryst. **A 26**, 608 (1970).
[28] P. M. Gehring, S.-E. Park, and G. Shirane, Phys. Rev. B **63**, 224109 (2001).
[29] P. M. Gehring, S. Wakimoto, Z.-G. Ye, and G. Shirane, Phys. Rev. Lett. **87**, 277601 (2001).
[30] S. Wakimoto, C. Stock, R. J. Birgeneau, Z.-G. Ye, W. Chen, W. J. L. Buyers, P. M. Gehring, and G. Shirane, Phys. Rev. B **65**, 172105 (2002).
[31] J. Toulouse and B. Hennion, Phys. Rev. B **49**, 1503 (1994).
[32] J. Hlinka, S. Kamba, J. Petzelt, J. Kulda, C. A. Randall, and S. J. Zhang, J. Phys.: Condes. Matter **15**, 4249 (2005).
[33] C. Stock, H. Luo, D. Viehland, J. F. Li, I. Swainson, R. J. Birgeneau, and G. Shirane, J. Phys. Soc. Jpn. **74**, 3002 (2005).
[34] J. J. van der Klink, D. Rytz, F. Borsa, and U. T. Höchli, Phys. Rev. B **27**, 89 (1983).
[35] C. Stock, D. Ellis, I. P. Swainson, G. Xu, H. Hiraka, Z. Zhong, H. Luo, X. Zhao, D. Viehland, R. J. Birgeneau, and G. Shirane, Phys. Rev. B **73**, 064107 (2006).
[36] W. Kleemann S. Kütz, and D. Rytz, Europhys. Lett. **4**, 239 (1987).